# Meta Neural Ordinary Differential Equations For Adaptive Asynchronous Control

#### Achkan Salehi

Sorbonne Université, achkan.salehi@sorbonne-universite.fr

#### Steffen Rühl

Magazino GmbH ruehl@magazino.eu

## **Stephane Doncieux**

Sorbonne Université, stephane.doncieux@sorbonne-universite.fr

**Abstract:** Model-based Reinforcement Learning and Control have demonstrated great potential in various sequential decision making problem domains, including in robotics settings. However, real-world robotics systems often present challenges that limit the applicability of those methods. In particular, we note two problems that jointly happen in many industrial systems: 1) Irregular/asynchronous observations and actions and 2) Dramatic changes in environment dynamics from an episode to another (*e.g.* varying payload inertial properties). We propose a general framework that overcomes those difficulties by meta-learning adaptive dynamics models for *continuous-time* prediction and control. We evaluate the proposed approach on a simulated industrial robot. Evaluations on real robotic systems will be added in future iterations of this pre-print.

**Keywords:** Meta-learning, Neural ODEs, Reinforcement Learning

# 1 Introduction

Machine Learning methods have increasingly been studied and applied for decision making and control in robotic systems during the past few years. Model-free Reinforcement Learning (RL) methods [1, 2, 3] have shown great success in various robotics tasks, and model-based Reinforcement Learning an Planning [4, 5] have garnered considerable attention due to their increased data-efficiency. More recently, population based methods such as model-free and model-based Quality-Diversity (QD) algorithms [6, 7] have also shown promise in contexts where behavioral diversity is essential.

However, the vast majority of those methods, if not all of them, have been applied in contexts where the difficulties and constraints present in real-world systems are partially relaxed. In particular:

- In a large number of systems, observations and actions are irregular/asynchronous. This contrasts
  with the assumptions made by the majority of works in RL/QD, in which actions are applied at a
  given state and observations are received at regular intervals.
- 2. The dynamics of the environments in which real-world systems operate, while often non-stationary during an episode, are also subject to dramatic discontinuous changes between episodes. This can be for example because of the change in the geometry or mass distribution of a payload, or an unexpected malfunction of some component.

Current work in RL/QD in general only handles one of those aspects, and robust methods for jointly addressing those problems are still lacking. For example, many systems that incorporate some notion of meta-learning [8, 2, 9], or system identification [3] are able to adapt to unseen tasks with minimal adaptation. However, to our knowledge, none of these methods address the problem of irregular actions and observations. Similarly, RL methods that are designed to handle those issues and/or operate in continuous-time scenarios [10, 11] are applied to environments that do not change significantly between episodes, and thus do not require much generalization. In contrast, we propose a more general framework that is capable of jointly handling both of the aforementioned problems, and that we have dubbed *ACUMEN*, for Adaptive Control in AsynchronoUs probleM sEttiNgs.

We take inspiration from the industrial robot SOTO, manufactured by Magazino GmbH<sup>1</sup>, which manipulates payloads of varying inertial properties. Based on that robot, we develop a simplified, light-weight pybullet [12] simulation which showcases the advantages of the proposed method.

The paper is structured as follows. The following section (§2) is dedicated to problem formalization and notations. We position our work with respect to the literature in §3 describe the proposed method in §4. Experimental results are presented in §5. System limitations and future directions are discussed in section §6. Closing remarks are the subject of §7.

## 2 Problem formulation and Notations

We consider robotic systems with irregular/asynchronous actions and observations that operate in episodic fashion such that the dynamic system governing state transitions during a given episode is sampled from an unknown distribution. We formalize those problems below.

Irregular/asynchronous actions and observations. In most of the RL literature, actions and observations are regular and synchronized: one performs an action  $a_t$  in some state  $z_t$ , and receives an observation  $\omega_{t+1}$ . In contrast, we are interested in the general case in which observations and actions are given as  $\omega_{t_1}, ..., \omega_{t_k}$  and  $a_{t'_1}, ..., a_{t'_l}$  with  $l \neq k, t'_i \neq t_i$ . Typically, there might be many actions between two observations, and vice-versa.

We frame such problems as Continuous Time, Partially Observable Markov Decision Processes (CTPOMDP) in which the observation function is time-dependent. More formally, we consider the tuple  $\mathcal{T}\triangleq < Z, \mathcal{A}, \mathcal{F}, R, \Omega, \Phi, \gamma, T >$  where  $Z\subset\mathbb{R}^N$  and  $\mathcal{A}\subset\mathbb{R}^M$  respectively denote the set of states and the set of actions. Let us denote  $\pi:\mathbb{R}\to\mathcal{A}$  the function defining the actions to be applied at time t. Then  $\mathcal{F}$  defines the evolution of the dynamic system:

$$z(t_0 + \Delta t) = z(t_0) + \int_{t_0}^{\Delta t} \mathcal{F}(z(t), t, \pi(t)) dt.$$
 (1)

The possible time intervals over which the system operates are noted T and the function  $\Phi: Z \times T \times \Omega \to [0,1]$  defines the probability  $p(\omega|z,t)$  of an element  $\omega$  of the observation space  $\Omega$  given a state-time pair. In what follows,  $a_t$  will denote an action applied at time t. Likewise,  $\omega_t$  will indicate an observation made at time t. The function  $R: Z \times \mathcal{A} \to \mathbb{R}$  is a dense reward function and  $\gamma \in (0,1]$  is a discount factor. During an episode associated to the tuple  $\mathcal{T}$ , our aim is to find  $\pi(t)$  that maximizes the discounted cumulative reward  $\int_0^\infty \gamma R(z(t),\pi(t))dt$ .

Changes in environment dynamics. We consider the case in which environment dynamics remain stationary through the duration of an episode, but dramatically and discontinuously change in between different episodes. More formally, each task  $\mathcal{T}$  is sampled from a distribution of the form

$$P(\mathcal{T}) = P(\langle Z, \mathcal{A}, \mathcal{F}, R, \Omega, \Phi, \gamma, T \rangle) \triangleq P(\mathcal{F}). \tag{2}$$

In other words, two episodes associated to two distinct tasks  $\mathcal{T}_i$ ,  $\mathcal{T}_j$  only differ in  $\mathcal{F}_i$  and  $\mathcal{F}_j$ , while the rest remains unchanged. An example of this is changes in the geometry and mass distributions of objects being manipulated by a robotic arm. Our objective is to find an adaptive control process  $\pi(t,\theta)$  parametrized by  $\theta$  that leverages previous learning experience to adapt to new, unseen tasks from  $P(\mathcal{T})$ .

#### 3 Related Work

**Model-based Reinforcement Learning and Control.** Model-based RL (MBRL) [13] with learned models has been demonstrated to be superior in terms of data-efficiency compared to model-free RL (MFRL), particularly in low-data regimes [14, 15, 4]. This is particularly important on robotic systems, where the large number of interactions required by model-free methods are often impractical. While it has been observed that MBRL can suffer from lower asymptotic performance compared to MFRL [15, 14], recent works [16] demonstrate that this performance gap can be closed by accounting for model uncertainty, which results in better exploration.

A popular approach to Model-based Control is to sample action-state trajectories from the learned model, for example via the Cross Entropy Method (CEM) [17, 5]. Each trajectory is then evaluated based on the predicted states, and the N first actions from the best trajectory are applied on the real system. As a population-based algorithm, the model-based CEM is robust to model inaccuracies, and has been shown to produce results that are on-par with MFRL [16, 18]. Furthermore, CEM, unlike most of the work based on learned policies, is not tied

<sup>&</sup>lt;sup>1</sup>https://www.magazino.eu

to a particular reward function: indeed, the reward function can be changed at any time during or in-between episodes, without any need for additional training. While vanilla CEM suffers from poor data-efficiency in high-dimensional spaces, recent efforts [5] demonstrate that this aspect can be significantly improved, in particular via sampling time-correlated action sequences.

We use CEM-based planning in this paper. In addition to the reasons that were enumerated above, our choice is also motivated by the method's simplicity, which allows us to focus on the main message of this paper: that combining neural ODEs with meta-learning results in a framework suitable for adaptive control in situations where actions and observations are asynchronous/irregular.

Irregular/asynchronous actions and observations and continuous time control. The vast majority of the RL literature considers discretized time-steps with regular observations and actions, and most prior work on continuous time systems make simplifying assumptions such as partially known and/or linearized dynamics systems [19, 20, 21], or are applied in model-free settings [22, 23]. However, more recent efforts build on Neural Ordinary Differential Equations (N-ODEs) which outperform discrete approaches to modeling continuous-time dynamics [24]. In their work, Du et al. [11] model environment dynamics using N-ODEs in order to learn policies in semi-MDP problem settings, while the continuous-time RL framework of Yildiz et al. [10] is notable for providing state uncertainty estimates. While our use of N-ODEs is similar to what was done in those works, it should be noted that our focus is on an orthogonal direction: our aim is to investigate the combination of meta-learning and N-ODEs in order to simultaneously address the problem of irregular/asynchronous actions and observations and discontinuous changes in system dynamics on a per episode basis. This distinction is reflected in our experimental setup, which is closer to real-world applications.

Meta-learning. Leveraging previous experience to improve the learning process has been extensively studied in the meta-learning [25, 26] literature. As even when considering the most restrictive definitions of meta-learning in which identical train/test conditions, end-to-end optimization and sample splitting are essential [25], one is left with a plethora of methods that differ, among other things, in what meta-parameters they optimize. For example, many meta algorithms learn a recurrent network that models policies [27] or optimizers/update rules [28], while others optimize hyperparameters [29] or metrics [30]. It is thus important to note that the meta-parameter that we seek to optimize is a prior dynamics model (more precisely, a neural ODE), which when used as an initialization in novel control tasks, should be able to quickly adapt to represent the dynamics of that environment. Learning adaptive priors is precisely what algorithms in the MAML family [8, 31] are designed for. In particular, we update our parameters in a manner similar to ES-MAML [31], as it alleviates the need for the estimation of second order neural ODE derivatives.

## 4 ACUMEN

We propose an algorithm based on Model Predictive Control (MPC) [5, 13] with a learned and dynamically adapted environment model based on the formalism of Neural Ordinary Differential Equations (N-ODE) [24]. In order to ensure performance on unseen tasks, learning experience from previous episodes is used to maintain a prior on the weights of the N-ODE with which each new episode is initialized. Each of the following subsections is dedicated to one of those components. An overview of our approach is given in algorithm 1.

## 4.1 Handling irregular/asynchronous observations and actions

As the state in the problem settings that we discussed in section §2 is partially observable, we assume the existence of a learned or hand-designed function  $\xi_n:\omega_0\times\omega_1\times...\times\omega_n\to Z$  that maps a sliding window of observations  $W=\{\omega\}_{i=1}^n$  to a state approximation, i.e.  $\xi(W)=\hat{z}\in Z$ . When clear from context, we will drop the window size from the notation and simply write  $\xi$ . We then use a neural ODE  $\hat{\mathcal{F}}$ , parametrized by weights  $\theta$  to approximate the dynamics evolution function  $\mathcal{F}$ :

$$\hat{z}(t_0 + \Delta t) \approx \hat{z}(t_0) + \int_{t_0}^{\Delta t} \hat{\mathcal{F}}(\hat{z}(t), t, \pi(t), \theta) dt.$$
(3)

As we are interested in irregular actions, the function  $\pi$  will in effect be the composition of two functions: a decision process  $u(t_0-s,t_0+\Delta t)$  that outputs irregular actions at discrete timestamp falling in some time interval, and an interpolation function that interpolates those actions to produce action values at continuous timestamps. More formally,  $\pi$  can be written as

$$\pi(t) = (\mathcal{I} \circ u(t_0 - s, t_0 + \Delta t))(t) \quad \forall t \in [t_0 - s, t_0 + \Delta t]$$

$$\tag{4}$$

for some (small) real value s. In our work, the interpolation  $\mathcal I$  is the linear interpolation function.

In our CEM-based system,  $N_p$  different action sequences, each of length H, are sampled and considered as possible continuations of the current history of actions. Each of these action sequences can be thought of as a

## **Algorithm 1:** The ACUMEN algorithm.

Input: Task distribution  $\mathcal{P}(\tau)$ , train/validation split ratio  $r_{split} \in (0,1)$ , maximum number of iterations for inner loop (neural ODE) optimizations  $N_{it}$ , optionally prior parameters of the N-ODE  $\theta_0$ , hyperparameters cem\_hyperparams for the CEM-based step (see algorithm 2), function  $\xi$  mapping sliding windows of observations to state approximations, size of sliding window of observations M

```
2 \theta \leftarrow \mathtt{RandomInit}() if \theta_0 is not given; else \theta \leftarrow \theta_0
 3 while session no over do
           // sample i.i.d vectors for the ES update of the meta-parameters
           \epsilon_1,...,\epsilon_N \sim \mathcal{N}(\boldsymbol{0},\boldsymbol{I})
           for i \in \{1, ..., N\} do
 5
                \tau_i \sim \mathcal{P}(\tau)
\mathcal{D}_i^{train} \leftarrow \emptyset
 6
                 \mathcal{D}_i^{val} \leftarrow \emptyset
                 \theta_i^* \leftarrow \theta + \epsilon_i \sigma
                 \hat{C}_{hist} \leftarrow \emptyset /\!/ history of applied actions
10
                 while not (\tau_i.success or \tau_i.timeout) do
11
12
                        // get the M most recent observations
                        \omega_1, ..., \omega_M = \tau_i. get\_sliding\_window(M)
13
                        // get all actions sent since the oldest observation in the window
                        c_1, ..., c_l=GetAllActionsSince(\omega_1.timestamp, C_{hist})
14
15
                        // Map the sliding window to a state approximation
                        \hat{z} = \hat{\xi}(\omega_1, ..., \omega_M)
16
17
                        // Choose the next action sequence (see algorithm 2 for details)
                        seq=CEMStep(\theta_i^*, \hat{z}, \{c_1, ..., c_l\}, cem_hyperparams)
18
                        // Apply the K first actions in the sequence
                        \tau_i.Apply(seq<sub>1:K</sub>)
19
                        // Add the applied actions to command history
                        C_{hist}.append(seq<sub>1:K</sub>)
20
21
                        // split gathered data into train/validation sets
                        \hat{d_{train}}, \hat{d_{val}} \leftarrow \text{sample\_split}(([\omega_1, ..., \omega_M], [c_1, ..., c_l], r_{split})
22
                        \mathcal{D}_{i}^{train}.append(d_{train})
23
                        \mathcal{D}_i^{val}.append(d_{val})
24
                        // optimize the prior if necessary
                        if train_freq then
25
                             \theta_i^* \leftarrow \text{OptimizeNODE}(\theta_i^*, \mathcal{D}_i^{train}, N_{it})
26
                        end
27
                 end
28
29
           // update the meta-parameters \boldsymbol{\theta}
          \theta \leftarrow \theta - \frac{\alpha}{N\sigma} \sum_{i=1}^{N} \mathcal{L}_i(\theta_i^*, \mathcal{D}_i^{val}) \epsilon_i
30
31 end
```

Algorithm 2: A single step of CEM based decision using neural ODEs. While predicted actions  $a_{1:H}^i$  are regularly sampled, their application on the system will be irregular. Thus, the history of actions  $c_1,...,c_n$  will be composed of irregularly applied actions, hence the advantage of using the neural-ODE formalism. Note that the action sequences sampled by SampleTimeCorrelatedSequence are time-correlated according to parameter  $\beta$ , as originally proposed in [5], and that the case of  $\beta=0$  is equivalent to sampling from a Gaussian distribution.

Input: Neural ODE weights  $\theta$ , state approximation  $\hat{z}(t_0)$  at time  $t_0$ , desired duration of state propagation  $\Delta t$ , previous actions  $c_1, ..., c_l$  (augmented with their timestamp info), mean and diagonal covariance  $\mu_0, \Sigma_0$ , population size Np, number of elites Ne, length of action sequence to sample H, reward function R(.), convergence criterion  $\mathcal{Y}$ , colored noise parameter  $\beta$ 

```
Output: action sequence a_1^*, ... a_H^*
1 Function CEMStep (\theta, \hat{z}(t_0), \{c_1, ..., c_l\}, \mu_0, \Sigma_0, N_p, N_e, H, R(.), \mathcal{Y}):
2
          \mu = \mu_0
         \Sigma = \Sigma_0
3
         // initialize elite set
         \mathcal{E} = \emptyset
4
         while not \mathcal{Y}(\Sigma) do
                // sample N_p action sequences of length H at regular intervals in [t_0, t_0 + \Delta_t]
                a_{1:H}^1,...,a_{1:H}^{N_p} \sim \texttt{SampleTimeCorrelatedSequence}(\mu, \Sigma, \beta)
6
                \quad {\bf for} \; {\it each} \; a^i_{1:H} \; {\bf do} \\
                      u_i = [c_1, ..., c_l].concatenate(a_{1:H}^i))
 8
                      // Let \pi_i(t) the function that computes actions via interpolating elements of u_i
                      \pi_i = \mathcal{I} \circ u_i
                      // propagate the state
                      \hat{z}_i = \hat{z}(t_0) + \int_{t_0}^{\Delta t} \hat{\mathcal{F}}(\hat{z}(t), \pi_i(t), \theta) dt.
// compute associated reward
10
                      r_i = \mathbf{R}(\hat{z_i})
11
                end
12
                \mathcal{E}=select best N_e action sequences according to the r_i
13
                \mu, \Sigma = fit Gaussian to \mathcal E
14
15
         // return the best action sequence (alternatively, re-sample using \mu, \Sigma after convergence)
         return \mathcal{E}
16
```

decision process  $u_i$  (with  $i \in \{1, ..., N_p\}$ ). Since the interpolation function  $\mathcal{I}$  is fixed, it is equivalent to say that the CEM method samples  $N_p$  functions  $\pi_i \triangleq \mathcal{I} \circ u_i$ .

### 4.2 Planning with a continuously updated model

The proposed method is based on Model Predictive Control (MPC) with a learned model, that is updated throughout the duration of an episode. At each iteration of the algorithm (lines 11-27 in algorithm 1), a sliding window consisting of the last M observations  $\{\omega_1,...,\omega_M\}$  is mapped to a state estimation  $\hat{z}(t)$ . Actions  $\{c_1,...,c_l\}$  (in general,  $l\neq M$ ) that have been applied since the time at which  $\omega_1$  was observed are gathered. All observations and actions are added to a buffer with the aim of updating the model.

We use the Cross Entropy Method [17] to determine an action sequence  $a_{1:H}^*$ , that when appended to  $\{c_1,...,c_l\}$ , would result in the most promising future state according the to the predictions of the learned model. The sampling and selection process is detailed in algorithm 2. As previously discussed in detail in section §3, our decision to rely on the CEM is not only motivated by its demonstrated efficacy and robustness, but also by its simplicity. Note that as proposed in recent works [5], the action sequences are sampled from a colored noise distribution with parameter  $\beta$ , which allows to adjust the time correlation of actions according to the task at hand, increasing the sample efficiency of the CEM method.

Once a sequence  $a_{1:H}^*$  has been selected, its first action is applied on the system. The learned model is updated every *train\_freq* iterations.

#### 4.3 Learning a neural ODE prior

Our objective of obtaining a point-wise estimate of weights that could serve as an adaptive prior in environments with previously unseen dynamics can be formulated via the following equation:

$$\theta \leftarrow \theta - \alpha \nabla \sum_{i=1}^{N} \mathcal{L}(\mathcal{T}_{val}^{i}, \theta - \lambda \nabla \sum_{j=1}^{N} \mathcal{L}(\mathcal{T}_{train}^{j}, \theta))$$
 (5)

in which  $\mathcal{L}(.,\theta)$  denotes the training loss of a neural ODE on some dataset. As is classically done in the metalearning literature for the sake of conciseness in notations, each of the inner and outer optimization problems have been written as a single gradient descent update. However, in practice the number of updates is arbitrary.

Notice that the inner optimization, *i.e.*  $\theta - \lambda \nabla \sum_{j=1}^{N} \mathcal{L}(\mathcal{T}_{train}^{j}, \theta)$ , corresponds to N model-predictive episodes (lines 11-28 in algorithm 1).

Computing the gradient update for the outer level optimization problem requires differentiating through the gradient computed in the inner optimization. As this would necessitate computing higher order derivatives of neural ODEs, we simplify the outer level update by using an estimator based on Evolution Strategies [32]:

$$\frac{1}{\sigma} \mathbb{E}_{\tau \sim P(\tau)} \mathbb{E}_{\epsilon \sim \mathcal{N}(0,I)} \mathcal{L}(\mathcal{T}_{val}^{\tau}, \theta + \epsilon - \lambda \nabla \mathbb{E}_{\tau \sim P(\tau)}^{N} \mathcal{L}(\mathcal{T}_{train}^{\tau}, \theta + \epsilon)) \epsilon. \tag{6}$$

Note that this update, approximated using N sampled environments in algorithm 1 (line 30) is equivalent to the zero-order ES-MAML update [31].

# 5 Experimental Validation

## 5.1 Simulation

As mentioned in the introduction, The robotic simulation that we have developed to evaluate ACUMEN is inspired by the SOTO robot manufactured by Magazino Gmbh. Before presenting our results, we detail the simulation in the following section. Results from the complete system are presented in section 5.1.2, and ablation studies follow in sections 5.1.3.

## 5.1.1 Simulation description

The simulation, developed using the bullet physics engine [12], defines the following problem: given two parallel and independently controlled conveyor belts separated by some distance (figure 1(a)), the aim is to rotate a parcel by  $\frac{\pi}{2}$  radians. The default problem setting is illustrated in figure 1(c). At the beginning of an episode, a box of varying inertial properties is sampled from a distribution  $P(\mathcal{T}_{box})$ , and is positioned (plus or minus some gaussian noise) at the pose shown in figure 1(c, left). The task is considered solved if the system reached (with some tolerance) the state given in the right hand of figure 1(c). The environment, shown in 1(b), is based on simulated roller conveyors [33].

The box distribution  $P(\mathcal{T}_{box})$  is defined by a random choice of mass in the interval [0.1kg, 3kg] and a mass distribution given by random 3d Gaussian distributions, which can have dense covariances. To simplify matters, we use ground truth 6d box poses as observations. Given the last two observed box poses  $\omega_{t-1}, \omega_t$ , we approximate the state to propagate as  $\hat{z} = [\omega_t, \frac{\omega_t - \omega_{t-1}}{\Delta t}]$ . Note that the action space is two-dimensional and defined by  $[-1,1] \times [-1,1]$ , as each of the conveyors can receive velocity controls independently of the other one. The distance from a given pose and the target pose is used as a dense reward signal to guide the CEM-based action selection process. For benchmarking purposes, we define each timestep as the time elapsed between applying actions in the physics engine, which is done at regular intervals. We however emphasize that those actions are not used by our control algorithm, which only receives actions that the result of linear interpolations at random time-steps. The maximum number of timesteps for each episode is set to  $H_{max} = 300$ .

In all experiments, the RK45 solver [34] (commonly referred to as dopri5) is used.

Irregular/asynchronous observations and actions. We simulate irregular/asynchronous observations and actions by 1- Returning only one random observation among  $K_s$  successive observations, 2- returning actions at randomly interpolated time-stamps in between real actions and 3) Discarding selected observations with some probability  $\eta$ . In the following experiments, a value of  $K_s=3$  has been chosen, and  $\eta=0.05$ . The colored noise parameter used in CEM-based sampling (algorithm 2 was set to  $\beta=2$ ).

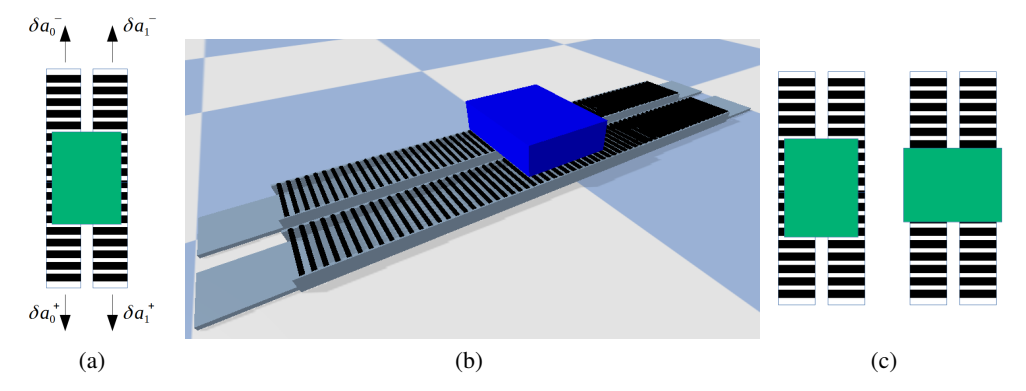


Figure 1: (a) Schematic view of the system, showing a green box on top of two conveyor belts. The conveyor belts are independent, and the motion of each one is controlled via a one-dimensional velocity command in [-1,1]. Positive and negative actions, e.g.  $\delta a_0^+, \delta a_0^-$  respectively move the left conveyor in the top or bottom direction. Commands such as  $\delta a_1^+, \delta a_1^-$  should affect the right-hand conveyor belt in similar fashion. (b) Screenshot of the developed robot simulation, based on simulating two roller conveyors. (c, left) Illustration of the initial conditions (making abstraction of small variations) in each episode. (c, right) Target pose that we aim to reach through controlling the conveyor belts. Note that the mass and inertial properties significantly and discontinuously vary in-between episodes.

## 5.1.2 Simulation: system results

The objective of this subsection is to validate the complete system in the presented simulation, where irregular/asynchronous actions and observations have been simulated, and where environment dynamics vary from one episode to the next due to the random sampling of box mass and inertial properties.

A neural ODE is initialized with random weights, and receives successive meta updates in order to form the learned prior. In each meta iteration, N=20 tasks  $\tau_1,...,\tau_N$  are sampled from the environment distribution. As detailed in algorithm 1, the neural ODE is independently adapted to each of the  $\tau_i$  using data gathered during the episode, the validation split of which is then used in the meta update.

The result of the experiment are plotted in figure 2. As figure 2(a) shows, at initialization, model-predictive control with the random neural ODE is only able to solve about 5% of the environments that are sampled from the test distribution. In this first meta iteration, the variance of episode lengths (figure 2(b)) is large, with most episode requiring many updates to the neural ODE. Hence, the large mean episode length reported in that same figure.

It can be seen that as the learned prior is optimized during successive meta-iteration, the percentage of successfully solved test environments increases until eventually reaching a point where it oscillates between 95-100% (figure 2(a)). Simultaneously, the number of steps spent across all environments (solved and unsolved) decreases as the optimization of the prior progresses (figure 2(b)).

Figure 2(c) shows the number of timesteps spent in environments that the system was able to solve at a given meta iteration. After an initial large drop in mean and variance in the first few (< 10) meta iterations, the number of necessary steps for solving an environment stabilizes to around 100 timesteps, while the number of success (figure 2(a)) continues to grow. A possible explanation for this phenomenon comes from observing the behavior of models specialized for an environment, an example of which will be discussed in the next subsection. Models that are specialized to an environment result in near-optimal state-action trajectories connecting the initial box pose to the target pose, and take about 40 to 50 timesteps. A general prior would then be positioned in some area of parameter space minimizing its average distance to several specialist networks, hence the higher number of updates necessary for its adaptation.

## 5.1.3 Simulation: Ablations

Our principal aim in this paper is to investigate the advantages of combining meta-learning and neural-ODEs in the contexts that were previously discussed. Therefore, we consider two ablation experiments. In the first one, we consider two different manners in which the meta-update component can be removed. In the second ablation study, we compare a specialized neural ODE to a specialized Recurrent network.

**Meta-update ablation**. We first naively disable the meta-update in ACUMEN. The results of this experiment are reported in figure 3. Unsurprisingly, without the meta update, the adaptations that the neural ODE goes

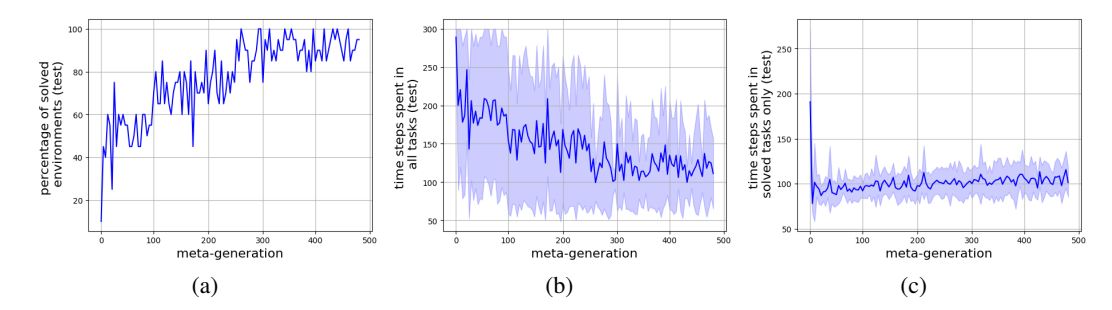


Figure 2: (a) The evolution of the percentage of solved environments among the  $M_{test}=20$  ones that are sampled from the test distribution  $P(\mathcal{T}_{box})$  at each meta-generation, starting from a random neural ODE. (b) In this figure, the value displayed at each meta-generation is the time spent in all tasks (solved and unsolved) that have been sampled at this meta-iteration. (c) Same as in (b), but for solved environments only. Notice the large drop in the number of necessary timesteps in the  $\sim 10$  first meta-generations.

through within distinct episodes is only sufficient for solving on average about  $\sim 9\%$  of the sampled tasks in the given time limit of  $H_{max}=300$  (which is the same as in all our simulation-based experiments). The number of timesteps solved in all environments (solved or unsolved) displays significantly higher mean and variance.

To further investigate the advantages of the learned prior, we compare its performance with that of a specialist model trained until convergence on a single "average" environment, henceforth noted  $E_1$ , given by a box with mass 1.5kg and uniform mass distribution. The results are compiled in table 1. As expected, the learned prior is able to adapt to and solve 91.3% of the environments within the (per episode) time limit of  $H_{max}$ , while the specialized model is able to solve 77.8% of the environments. The number of timesteps spent across all environments has lower mean and standard deviation  $\mu_{time}$ ,  $\sigma_{time}$  when the learned prior is used. It is however interesting to note that the specialized model can more easily solve environments that are close to the task it has been trained for. This is why  $\min_{time}$ , the minimum number of necessary timesteps across all environments is lower for the specialized environment in table 1.

	#sampled environments	success	$\mu_{time}$	$\sigma_{time}$	$\min_{time}$
learned general prior	600	548 (91.3%)	121.943	57.85	58
specialized model	600	467 (77.8%)	127.513	92.26	40

Table 1: Comparison between the prior learned by ACUMEN and a specialized model trained in an average environment on 600 randomly sampled boxes. Here,  $\mu_{time}$ ,  $\sigma_{time}$  denote the mean and average of the number of timesteps spent in a given environment, which are both lower for the learned prior. The minimum number of time-steps used to solve an environment is denoted  $\min_{time}$ .

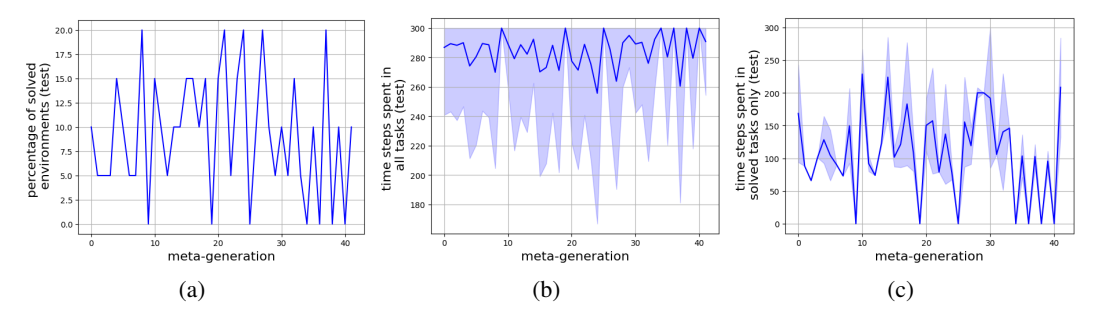


Figure 3: Result of meta-update ablation. (a,b). It can be seen that a random neural ODE can be adapted to solve an average of 9% of the sampled environments in the given time limit of  $H_{max}=300$ . Naturally, disabling the meta-update (c) The average and the variance of time-stamps spent in solved environments is much higher than with the learned prior.

	Neural ODE	RNN
#episodes	30	30
success	24 (80%)	15 (50%)
$\mu_{time}$	58.125	109.26
$\sigma_{time}$	10.89	34.93
$med_{time}$	59.15	107.0

Table 2: Comparison between a specialized neural ODE and a specialized RNN.

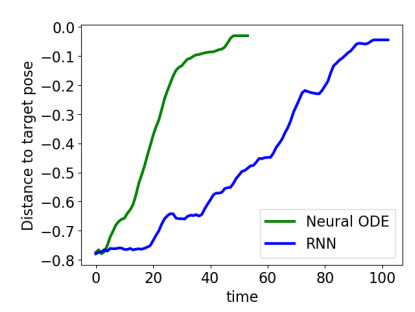


Figure 4: Comparison between typical trajectories resulting from neural ODEs vs RNNS.

**Neural-ODE ablation.** Classical model-based RL approaches usually learn a model of the form  $z_{t+1} = M(z_t, a_t)$ , which corresponds to (PO)MDPs. A simple extension to that model for the case of irregular/asynchronous actions can be obtained by considering a recurrent neural network with some representation of z(t) as its initial state, which would take as input the sequence of tuples  $(a_0, \Delta t_0), ..., (a_n, \Delta t_n)$  with  $\Delta t_i$  the elapsed time between  $a_i$  and  $a_{i+1}$  for  $i \neq n$ , and  $\Delta t_n$  the elapsed time between  $a_n$  and the next observation (or during planning, the next predicted state). In this paper, we implement this model as a vanilla stacked RNN of depth 5. Note that this is a slight generalization of state propagation of the form  $z_t = z_{t-1} + M(z_{t-1}, a_{t-1}, \Delta t_{t-1})$  which was shown in prior work [10] to be inferior to neural ODEs in continuous time settings.

For this experiment, we considered an environment with fixed dynamics, that we will note  $E_2$ , corresponding to a mass of 0.5kg and uniform mass distribution. The stacked RNN was first pretrained on data from that environment, which were gathered from three episodes with significant action-state coverage: one with random controls, one successful episode with neural-ODE based control, and another episode using the same neural-ODE but with noise injected into the actions. It was then compared during 30 model-predictive trials to the specialist neural-ODE model that was learned in the previous section on the  $E_1$  environment. Note that while the dynamic system is fixed, the observations and actions change from one episode to the other, as they are the result of interpolations at random timestamps, as previously specified in section §5.1.1. The results are reported in table 2.

It can be seen that the ODE-based network, specialized for the  $E_1$  environment, performs significantly better than the recurrent model on the  $E_2$  model, for which the latter is a specialist. This is expected, as the recurrent model is equivalent to linearizing the dynamics model on a much coarser scale than what an ODE solver would do. Figure 4 shows two example box pose trajectories from successful episodes, one obtained using the neural ODE (in green), and the other from using the recurrent model (blue curve). Each curve represents the distance from the current pose to the target state. It can be seen that the trajectory obtained with the neural ODE is much smoother than the one resulting from the stacked RNN.

# 6 Discussion

The experiments above have clearly demonstrated the advantages of the proposed approach in systems with irregular/asynchronous observations and actions, where system dynamics can dramatically and discontinuously change from an episode to the next. However, the current implementation of the proposed method suffers from the computational overhead caused by the CEM-based sampling, which makes the system unsuitable for high frequency control. While a potential solution to this problem could be to plan with learned policies conditioned on the dynamics, one should also consider the trade-offs between accuracy and speed that result from the choice of a particular ODE solver.

Experiments with real robotic systems will be added to future iterations of this preprint.

## 7 Conclusion

Motivated by challenges encountered in industrial robotic systems, we proposed a method for Model Predictive Control that handles significant changes in environment dynamics in-between episodes, in settings where observations and actions are irregular/asynchronous. The solution, which combines meta-learning with neural ODEs, was validated in a simulation inspired by a real robotic system. Experiments with real robotic systems will be added to future iterations of this preprint.

#### Acknowledgments

This work was supported by the European Union's H2020-EU.1.2.2 Research and Innovation Program through FET Project VeriDream under Grant Agreement Number 951992. We wish to thank Quentin Levent for their initial work on the simulation. Likewise, we express our gratitude to Patrick Gallinari and Yuan Yin for their valuable input and criticism during the development of the presented material.

## References

- [1] S. Levine, P. Pastor, A. Krizhevsky, J. Ibarz, and D. Quillen. Learning hand-eye coordination for robotic grasping with deep learning and large-scale data collection. *The International journal of robotics research*, 37(4-5):421–436, 2018.
- [2] I. A. OpenAI, M. Andrychowicz, M. Chociej, M. Litwin, B. McGrew, A. Petron, A. Paino, M. Plappert, G. Powell, R. Ribas, et al. Solving rubik's cube with a robot hand. 2019.
- [3] A. Kumar, Z. Fu, D. Pathak, and J. Malik. Rma: Rapid motor adaptation for legged robots. *arXiv preprint arXiv:2107.04034*, 2021.
- [4] M. Deisenroth and C. E. Rasmussen. Pilco: A model-based and data-efficient approach to policy search. In *Proceedings of the 28th International Conference on machine learning (ICML-11)*, pages 465–472, 2011.
- [5] C. Pinneri, S. Sawant, S. Blaes, J. Achterhold, J. Stueckler, M. Rolinek, and G. Martius. Sample-efficient cross-entropy method for real-time planning. arXiv preprint arXiv:2008.06389, 2020.
- [6] B. Lim, L. Grillotti, L. Bernasconi, and A. Cully. Dynamics-aware quality-diversity for efficient learning of skill repertoires. *arXiv* preprint *arXiv*:2109.08522, 2021.
- [7] S. Kim, A. Coninx, and S. Doncieux. From exploration to control: learning object manipulation skills through novelty search and local adaptation. *Robotics and Autonomous Systems*, 136:103710, 2021.
- [8] C. Finn, P. Abbeel, and S. Levine. Model-agnostic meta-learning for fast adaptation of deep networks. In *International conference on machine learning*, pages 1126–1135. PMLR, 2017.
- [9] A. Salehi, A. Coninx, and S. Doncieux. Few-shot quality-diversity optimisation. *arXiv preprint* arXiv:2109.06826, 2021.
- [10] C. Yildiz, M. Heinonen, and H. Lähdesmäki. Continuous-time model-based reinforcement learning. In International Conference on Machine Learning, pages 12009–12018. PMLR, 2021.
- [11] J. Du, J. Futoma, and F. Doshi-Velez. Model-based reinforcement learning for semi-markov decision processes with neural odes. Advances in Neural Information Processing Systems, 33:19805–19816, 2020.
- [12] E. Coumans and Y. Bai. Pybullet, a python module for physics simulation for games, robotics and machine learning. http://pybullet.org, 2016–2021.
- [13] T. M. Moerland, J. Broekens, and C. M. Jonker. Model-based reinforcement learning: A survey. arXiv preprint arXiv:2006.16712, 2020.
- [14] L. Kaiser, M. Babaeizadeh, P. Milos, B. Osinski, R. H. Campbell, K. Czechowski, D. Erhan, C. Finn, P. Kozakowski, S. Levine, et al. Model-based reinforcement learning for atari. arXiv preprint arXiv:1903.00374, 2019.
- [15] A. Nagabandi, G. Kahn, R. S. Fearing, and S. Levine. Neural network dynamics for model-based deep reinforcement learning with model-free fine-tuning. In 2018 IEEE International Conference on Robotics and Automation (ICRA), pages 7559–7566. IEEE, 2018.
- [16] K. Chua, R. Calandra, R. McAllister, and S. Levine. Deep reinforcement learning in a handful of trials using probabilistic dynamics models. *Advances in neural information processing systems*, 31, 2018.
- [17] R. Rubinstein. The cross-entropy method for combinatorial and continuous optimization. *Methodology and computing in applied probability*, 1(2):127–190, 1999.
- [18] D. Hafner, T. Lillicrap, I. Fischer, R. Villegas, D. Ha, H. Lee, and J. Davidson. Learning latent dynamics for planning from pixels. In *International conference on machine learning*, pages 2555–2565. PMLR, 2019.

- [19] J. Lee and R. S. Sutton. Policy iterations for reinforcement learning problems in continuous time and space—fundamental theory and methods. *Automatica*, 126:109421, 2021.
- [20] M. Abu-Khalaf and F. L. Lewis. Nearly optimal control laws for nonlinear systems with saturating actuators using a neural network hjb approach. *Automatica*, 41(5):779–791, 2005.
- [21] H. Wang, T. Zariphopoulou, and X. Y. Zhou. Reinforcement learning in continuous time and space: A stochastic control approach. J. Mach. Learn. Res., 21(198):1–34, 2020.
- [22] C. Tallec, L. Blier, and Y. Ollivier. Making deep q-learning methods robust to time discretization. In *International Conference on Machine Learning*, pages 6096–6104. PMLR, 2019.
- [23] M. Ghavamzadeh and S. Mahadevan. Continuous-time hierarchical reinforcement learning. In *ICML*, volume 18, pages 186–193, 2001.
- [24] R. T. Chen, Y. Rubanova, J. Bettencourt, and D. K. Duvenaud. Neural ordinary differential equations. Advances in neural information processing systems, 31, 2018.
- [25] T. Hospedales, A. Antoniou, P. Micaelli, and A. Storkey. Meta-learning in neural networks: A survey. arXiv preprint arXiv:2004.05439, 2020.
- [26] T. Schaul and J. Schmidhuber. Metalearning. Scholarpedia, 5(6):4650, 2010. doi:10.4249/scholarpedia. 4650. revision #91489.
- [27] Y. Duan, J. Schulman, X. Chen, P. L. Bartlett, I. Sutskever, and P. Abbeel. Rl <sup>2</sup>: Fast reinforcement learning via slow reinforcement learning. *arXiv* preprint arXiv:1611.02779, 2016.
- [28] J. Oh, M. Hessel, W. M. Czarnecki, Z. Xu, H. P. van Hasselt, S. Singh, and D. Silver. Discovering reinforcement learning algorithms. Advances in Neural Information Processing Systems, 33, 2020.
- [29] Z. Xu, H. van Hasselt, and D. Silver. Meta-gradient reinforcement learning. arXiv preprint arXiv:1805.09801, 2018.
- [30] O. Vinyals, C. Blundell, T. Lillicrap, D. Wierstra, et al. Matching networks for one shot learning. Advances in neural information processing systems, 29:3630–3638, 2016.
- [31] X. Song, W. Gao, Y. Yang, K. Choromanski, A. Pacchiano, and Y. Tang. Es-maml: Simple hessian-free meta learning. arXiv preprint arXiv:1910.01215, 2019.
- [32] T. Salimans, J. Ho, X. Chen, S. Sidor, and I. Sutskever. Evolution strategies as a scalable alternative to reinforcement learning. *arXiv* preprint arXiv:1703.03864, 2017.
- [33] P. M. McGuire. Conveyors: application, selection, and integration. CRC Press, 2009.
- [34] J. R. Dormand and P. J. Prince. A family of embedded runge-kutta formulae. *Journal of computational and applied mathematics*, 6(1):19–26, 1980.